International Journal of Osteoarchaeology
Int. J. Osteoarchaeol. **11**: 415–432 (2001)
DOI: 10.1002/oa.583

Destruction of Microstructure in Archaeological Bone: a Case Study from Portugal

MARY JACKES[a,*], RICHARD SHERBURNE[b], DAVID LUBELL[a], CHRISTINA BARKER[c] AND MICHAEL WAYMAN[c]

[a] *Department of Anthropology, 13–15 H.M. Tory, University of Alberta, Edmonton, Canada*

[b] *Department of Medical Microbiology and Immunology, 141 Medical Sciences, University of Alberta, Edmonton, Canada*

[c] *Department of Chemical and Materials Engineering, 536 Chemical/Mineral Engineering, University of Alberta, Edmonton, Canada*

ABSTRACT Sampling of archaeological human bone may not be justified, contrary to former high expectations regarding adult age assessment based on histomorphometry. The alterations in buried bone as a result of bacterial action are readily visible in the scanning electron microscope (SEM). An understanding of the chemical and structural changes to cortical bone requires work at the level of a few microns. This paper reports on problems encountered during analyses of samples of human bone from Mesolithic (ca. 8000 calBP) shell midden sites at Muge in central Portugal, and the methods used to try and overcome these problems. We believe we have shown that these Mesolithic bones are partly comprised of bacterially reprecipitated mineral, which has had collagen removed, with consequent obliteration of bone microstructure. We conclude that microbial destruction of the structure of archaeological bone can be a serious impediment to analysis of the characteristics of the population represented by those skeletal remains.

Key words: adult age assessment; bone microstructure; *Clostridium*; Mesolithic; Neolithic; Portugal

Introduction

In 1983, a reviewer of our successful grant proposal on 'The Mesolithic–Neolithic Transition in Southern Portugal' (cf. Lubell *et al.*, 1994), insisted that cortical bone remodelling analysis would provide accurate adult age assessment, and encouraged us to include it in our research design. This was entirely reasonable in light of the work being done at the time, which culminated in Uytterschaut's (1985) demonstration of an almost perfect correlation between adult age and the percentage of osteonal bone.

* Correspondence to: Department of Anthropology, University of Alberta, Edmonton, AB T6G 2H4 Canada. e-mail: Mary.Jackes@ualberta.ca

Materials and methods

The samples discussed here were taken from collections of Mesolithic and Neolithic human skeletal material held at the Serviços Geológicos in Lisbon, the Instituto Antropológico Mendes Correia in Porto, which have now been transferred to the University of Coimbra, and from two sites excavated by Zilhão (1984, 1992). A list of sites and their dates is provided in Table 1, and further details on these sites can be found in Lubell *et al.* (1994) and Jackes *et al.* (1997).

Following the example of Bocquet-Appel *et al.* (1980), we designed and had made two diamond-studded tungsten steel bits, which we mounted in a high speed rotary drill and used,

Received 10 April 2000
Revised 15 June 2000
Accepted 9 November 2000

Table 1. Chronology of Portuguese sites discussed in text

Site and period	Range in years, calBP
Mesolithic	
Moita do Sebastião	7597–8037
Cabeço da Arruda	7224–7783
Samouqueira	7224
Neolithic	
Caldeirão NA1	6668–6810
Caldeirão NA2	6965–7225
Furninha	estimated 5500–6900
Casa da Moura	5595–6869
Melides (Lagares Cave)	6144
Melides (Zambujal Cave)	4989
Feteira	4660–5297
Fontainhas	4724

with water cooling, to extract 9 mm diameter cores from the anterior femoral mid shaft. A first series of extractions from Moita do Sebastião (hereafter Moita) femora in the collections of the Serviços Geológicos, Lisbon, was done in 1984.

Because of concerns that heat and pressure during core removal were altering bone microstructure, a second series of samples from Cabeço da Arruda (hereafter Arruda) femora, also in the collections of the Serviços Geológicos, Lisbon, was removed in 1986 by making two cuts 4 mm apart using a rigid-backed, fine-toothed lapidary saw, and breaking out the resulting section by gentle torsion.

Despite numerous tests of different methods, no method was found which produced consistently readable sections from these samples. In part, the problems derived from an error on the part of Struers' representative in Lisbon, who provided Serefix instead of Epofix, an error which cannot be easily reversed (personal communication, Struers Copenhagen Export Department, 1.vii.87). Further work in Edmonton, using a variety of methods, showed that decalcification of bone samples led to destruction of the bone microstructure, and we found it was almost impossible to produce readable sections, despite the excellence of both the technicians and their equipment.

Great differences in hardness and softness were encountered. This was quantified roughly for the 9 mm cores by noting the time taken during standardized production of thin sections for 33 femora. A 64% coefficient of variation in the mean number of seconds taken (190) to cut a core, and the absence of significant correlation with any other observation (apart from one of two readings of periosteal porosity), indicates very clearly the variability and unpredictability of this factor.

It is now recognized that osteon counting may be an important element in accurate age estimation for younger adults, but, as with other age assessment methods, there is a cut-off point in accuracy and older adults will not be given accurate ages (see discussion in Jackes, 2000). A more important drawback, except in forensic cases, is the question of bone diagenesis (Jackes, 1992, p. 203). Palmer (1987) and Jackes (1992) discuss problems with the use of transmitting light, fluorescing light and polarized light microscopy in the examination of the Portuguese archaeological material (see also Jackes & Lubell, 1992, p. 264). Even much younger material, from coffins in church crypts, may be so altered as to be unreadable (Aiello & Molleson, 1993). In fact, Uytterschaut (1992) describes the difficulty of finding suitable femoral cortex, even within a dissecting room sample. Our discussion on the age of femoral samples from Gruta do Caldeirão (Jackes & Lubell, 1992, pp. 264–265) gives an idea of the limitations imposed by the destruction of cortical bone microstructure.

Porosity

Because cortical porosity (here defined as the number of resorption spaces) and density are also indicators of age, these must be considered in a discussion of whether bone sampling is valuable in archaeological contexts.

Porosity was quantified for Moita femoral cortices by counting the number of spaces between 80 and 400 μ in size within a number of 0.92 mm^2 areas (four to eight areas, see Palmer, 1987). This was done under fluorescing light, which allows visualization of organic material only, that is, intrusive calcite does not obstruct the field of analysis. Two readings were taken at 1-month intervals across the periosteal and mid-cortical areas, and three readings were taken across the endosteal cortex. Table 2 shows that periosteal porosity is highest, and endosteal porosity lowest.

Table 2. Porosity in femoral sections from Moita do Sebastião

Porosity	Mean *n* of spaces per 0.92 mm^2	*n*	S.D.
Periosteal	11.32	30	1.954
Midcortical	10.38	30	1.454
Endosteal	9.29	29	1.616

All three measures of porosity are significantly different from each other, and only periosteal and midcortical porosity are significantly correlated, ($r = 0.681$).

The difference between the outer two thirds of the cortex and the inner one third may be relevant because endosteal porosity alone appears correlated with age. There is no simple way of assessing the age of an adult skeleton (Jackes, 1992, 2000), but we find a consistent relationship between the Bergot & Bocquet (1976) method of evaluating age changes in the trabeculae of the proximal femur and the number of resorption spaces in the endosteal third.

Pfeiffer *et al*. (1995) show that assessment of the percent of remodelled bone will differ across the cortex, depending upon the location within the femoral cross-section, from the periosteal towards the endosteal area. Pfeiffer (1998) has pointed out that osteon and Haversian canal sizes are extremely variable within one sample of bone cortex. It has also been shown—based on 180 left femoral midshafts of individuals aged 21 to 97—that the amount of intracortical porosity is variable and a poor indicator of age (Feik *et al*., 1997).

It is not surprising then, that we found great variability within a sample. Based on the second count of the periosteal, medial and endosteal lines, the number of resorption spaces in each 9 mm core from Moita varied across the bone cortex, not only from outer to inner, but also from side to side. Overall, there was no significant difference between the lateral and medial margins of the 31 cores examined, but neither was there any correlation between the two margins in terms of porosity. Differences between sides of the core, in terms of magnitude and direction of difference, were not controlled by side, age or sex, whether the femur sampled was right or left, adult or subadult, male or female.

One indication, based on the nine extreme cases, is worth exploring in more detail: it is possible that young adults, having less porosity, also have far less porosity towards the lateral femoral cortex, while older adults, with greater porosity, have the reverse—that is, less porosity in the anterior femoral cortex medial to the midline. As Lazenby (1986) has pointed out, mid-cortical porosity is not completely random.

Density

Endosteal readings of the number of resorption spaces consistently had a non-significant positive correlation with density, while periosteal and midcortical porosity were both correlated negatively, again non-significantly, with density.

One might assume, then, that in these archaeological femoral samples, endosteal porosity has greater biological meaning than periosteal and midcortical porosity. Density was measured as weight (g) over volume (cc), with volume determined by displacement. Jackes & Lubell (1999, Table 1) demonstrate the curious fact that in adult males and females, the density of Arruda left femoral mid shaft cortex is greater than for Moita samples. Both sites are shell middens, in the same geological and geomorphological settings, so major differences in post-depositional processes seem unlikely. Cortical width (measured directly on bone samples) and Nordin's Index (measured on radiographs) shows that Moita femora have greater cortical thickness than Arruda femora, especially for females (Jackes & Lubell, 1999, Figures 1 and 2). There are low but significant negative correlations between femoral cortical density and cortical width measures in these samples. The implication is that the density of archaeological bone can be taken to mean something.

Nevertheless, Jackes (1992) noted that the mean femoral cortical density of 1.51 for the overall sample (Mesolithic and Neolithic) of 105 cores and sections was too low to be regarded as biologically meaningful, and this is particularly true of Moita adults, with a mean femoral cortical density of 1.19 ($n = 25$, S.D. $= 15$). We conclude, therefore, that burial

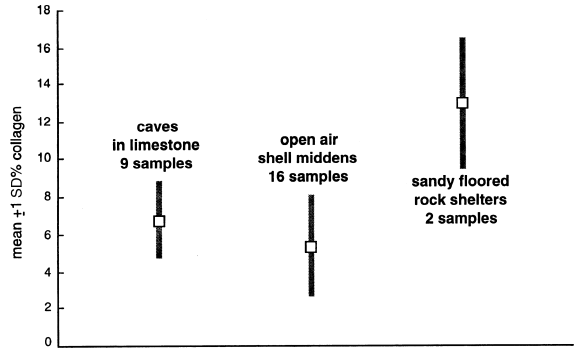

Figure 1. Percentage of collagen found in bone from different burial environments.

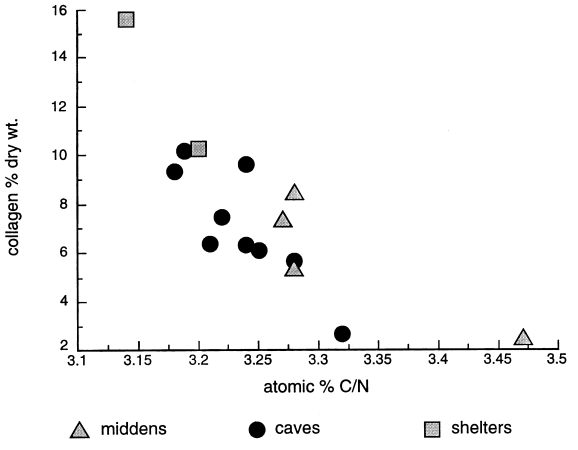

Figure 2. Atomic % C/N ratios plotted against % collagen for burial environments. Middens are Mesolithic, caves and shelters are Neolithic.

environment alters cortical density, as shown in Table 3.

Bedrock in the area of Melides, the location of the two sandy floored caves Zambujal and Lagares, is limestone, but the bones are not covered with calcium carbonate as they are at Caldeirão and Feteira (the two limestone caves in Table 3—Feteira is in a karstic formation and Caldeirão is a deep inland cave). Samples of matrix and soil (< 2 mm fraction) adhering to bones from Zambujal and Arruda have been analysed by X-ray diffraction (XRD) and also by spectrum analysis (EDAX elemental analysis by energy dispersive X-ray analysis), after many unpolished and uncoated samples of matrix and bone from several sites had been initially examined in 1985 using a Cambridge Stereoscan 250. The Feteira matrix sample suggests a clay (smectite—which swells significantly in contact with water), and granulometric analysis for that level (Zilhão, 1984) demonstrated at least fine silty deposits with 54% below 0.062 mm. Caldeirão deposits are characterized as sand and clay (Zilhão, 1992). Sand and clay are also suggested by analyses of fragments of breccia adhering to Casa da Moura teeth (Strauss *et al.*, 1988). Zambujal matrix and fine fraction analyses are dominated by quartz sand and feldspar—certainly potassium aluminium silicate (microcline). In fact, however, the spectra for Zambujal and Arruda fine fractions do not differ greatly (Si, K, Fe, Ti, Al, Mg, Cu, with variable amounts of Ca, depending on the source of the sample), not unexpected given their geological setting (Serviços Geológicos de Portugal, 1969).

While it is clear that no simple conclusions on bone preservation based on soil and drainage can be reached (Grupe, 1995; Nicholson, 1998), Table 3 suggests that the deeper caves (humid environments, but with stable conditions) did not provide a better situation for preservation of bone microstructure than the open-air shell middens. The shallow caves at Melides provide the best preservation environment.

This is supported by Figure 1, which demonstrates that the percentage of collagen retained (from the *in vivo* value of 18–20%) is greatly reduced in humid and/or non-stable environments.

Table 3. Comparison of the density of femoral cortical samples from different burial environments

Deposit type	*N*	Mean density	S.D.	*F*	*p*	*t*	*p* (two-tailed)
Shell midden	72	1.620	0.323				
Limestone cave	24	1.526	0.405	1.73	0.192	1.145	0.255
Shell midden	72	1.620	0.323				
Sandy floored cave	16	1.884	0.364	0.942	0.334	−2.888	0.005
Limestone cave	24	1.526	0.405				
Sandy floored cave	16	1.884	0.364	0.030	0.863	−2.845	0.007

The atomic % C/N ratio is higher when collagen percentage dry weight is lower. It is notable that one Arruda sample (Arruda III) which had only 2.56% collagen dry weight, stands out as having a high atomic % C/N ratio, and we could expect the same for those Moita bone samples which had poor collagen preservation (H. Schwarcz and M. Knyf, personal communications).

There is, however, no simple relationship between collagen preservation and bacterial activity. One sample from Furninha provided no collagen at all and, despite several attempts using scanning electron microscopy (SEM) (polished and uncoated, and gold coated), we were unable to find any evidence of microbial destruction. We do see a trend towards higher atomic C/N ratios in well preserved bone (see also Pate, 1998): while discussions with H. Schwarcz suggest a fair degree of confidence that 'there is no apparent trend to higher or lower isotope ratios' in comparing 'bones which have radically different levels of degradation' (personal communication 22.xii.99, contra Balzer *et al*., 1997), it is also evident that the C/N ratios of the extracted collagen are not perfect indicators of microbial activity.

We have, then, no simple way of assessing the preservation of bone microstructure, and we have very basic questions about the value of human bone histomorphometry in archaeological contexts, particularly when attempting comparisons among sites. Our large number of bone samples have not provided accurate adult ages because it has been impossible to undertake the histological methods of age assessment. The reason for this is discussed below.

Evidence for bacterial destruction of bone micromorphology

Jackes (1990) and Jackes *et al*. (1992) presented evidence in support of Baud & Lacotte (1984), that the postmortem destruction of bone microstructure is caused by bacterial action, not by fungal tunnelling. The human skeletal remains from Moita and Arruda appeared well-preserved, but examination of the femoral cortex thin sections showed advanced decomposition. The solubility of hydroxyapatite decreases in deposits with a high pH, and tests on breccia adhering to the bones showed it to be alkaline (two pH values of 9.55 and 9.58 were obtained from samples of breccia adhering to Arruda human femora 2037 and DR, respectively). The bedrock is limestone, but a more important factor is the amount of crushed estuarine shell in the sand and clay of the deposits. While bone mineral may be preserved in such an environment, bacterial preferences for alkaline surroundings may increase collagen destruction. We hypothesized (Jackes, 1990) that coccoidal bacteria remove collagen from solubalized compactum, reprecipitating bone mineral in a more dense form.

A Japanese experiment involving the burial of human bone for periods up to 15 years (Yoshino *et al*., 1991) proved that focal destruction is the result of bacterial action. These researchers did not characterize changes to the bone caused by bacterial action, but investigation of the micromorphology of Portuguese Mesolithic bone, led to the discovery of bacteria (Palmer, 1987) which encouraged us to concentrate on this question.

These bacteria (Figure 3) could not be isolated from bone scrapings (after freezing it was not possible to rehydrate the bacteria despite

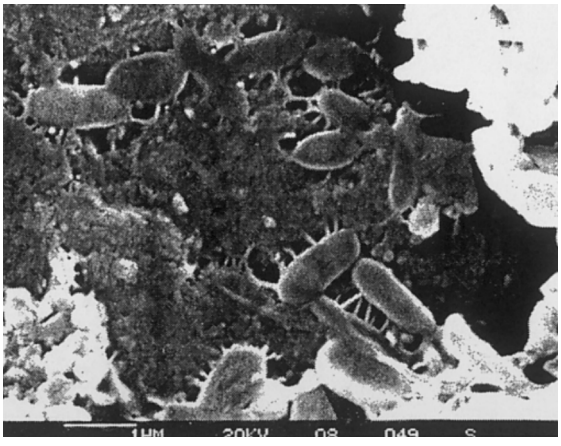

Figure 3. Scanning electron micrograph of unidentified bacteria on an uncut, coated surface of an unlabelled humerus from the Muge collections in the Institute of Anthropology, University of Porto (from original in Palmer, 1987, using Cambridge Stereoscan 250 equipped with a Kevex 7000 energy dispersive X-ray in an SEM, scale = 1 μ).

use of cryoprotectant), so identification was tentative. The bacteria appear to be *Clostridium*, 0.5–0.8 μ broad and 1.5 μ long, with peritrichous flagellae, whip-like extensions all over the cell surface. *Clostridium* is an anaerobic bacterium, occurring in soil and in the intestines of humans and other mammals. Using embedded, polished thin sections with a carbon coating, many attempts were made to visualize bacterial bodies and to understand the nature of the changes in the bone.

In a typical area (Figure 4), unaltered bone will be adjoined by the bright rim surrounding the bacterial colony: within the central destructive focus there are a few larger holes above 1 μ in diameter, many bacterial cavities have a slightly oval shape with a mean breadth of just under 1 μ, and are oriented so that the long axes of the cavities parallel each other. There are other smaller and less distinct holes which are close to 0.5 μ in diameter.

In the cross-section, illustrated in Figure 4, a sample of 80 holes was measured using Scion Image (1998). The measured holes all occupy the colony in the lower right hand of the image, and they have a mean breadth across the image, corresponding to the minimum diameter, of 0.97 μ, (S.D. = 0.22, range = 0.62–2.12). It seems likely that the few larger holes indicate the presence of spores, oval bodies which form in one end of a bacterial cell and swell it. In association with the oval form of the smaller holes, this indicates that *Clostridium* is a better identification than any coccoidal bacteria.

The best known bacteria which attack bone are *Clostridium histolyticum* (the species name means 'tissue dissolving'). *C. histolyticum* produces collagenase, the enzyme capable of digesting collagen. The diagnostic features of this species include a number of characteristics we have now been able to deduce from the Mesolithic bone: motile and peritrichous straight rods, 0.5–0.9 μ across, 1.3–9.2 μ long, occurring singly and side-by-side, in pairs or in short chains, and producing oval spores that cause the cell to bulge. The bacteria form fairly irregularly shaped colonies, sometimes described as 'fluffy or arborescent', sometimes circular, up to 2 mm across.

We are able to identify a number of areas on several samples with elongated cavities. The bacterial colonies have a complex though circumscribed form and contain tunnels. The tunnel trajectories vary, sometimes straight, sometimes quite tortuous, and dog-legged in a way congruent with chains of bacteria. In Figure 5, colonies around an Haversian canal are both

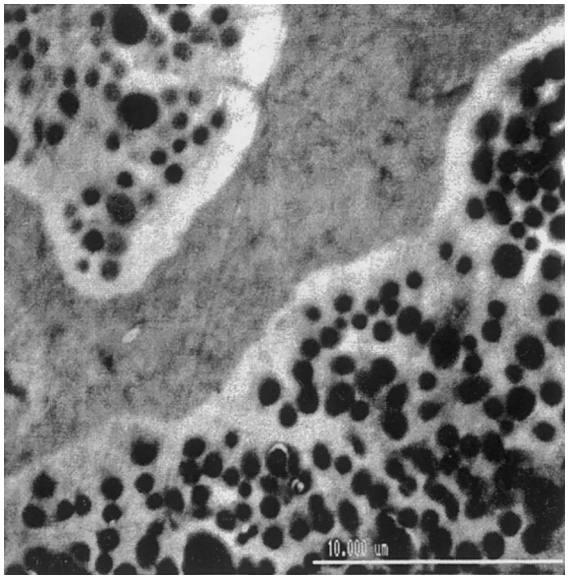

Figure 4. Polished uncoated thin section of left femoral cortex from Arruda 63 (sample 38), showing unaltered bone in the centre and bacterial colonies on either side (scan 8 on 24.viii.93, using Hitachi S-2700 SEM, scale = 10 μ).

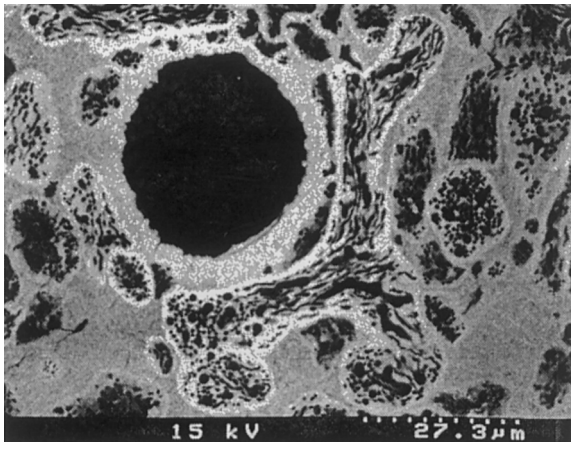

Figure 5. Backscattered electron image of left femoral cortex from Arruda 63 (sample 38) showing bacterial colonies around an Haversian canal in cross-section and longitudinally (24.viii.93, Hitachi S-2700 SEM, polished uncoated thin section, scale = 27.3 μ).

cross-sectioned and sectioned longitudinally, clearly showing the path of the larger tunnels extending through the colonies. The Haversian canal here is 36.5 by 32 μ across, slightly occluded because the canal walls are coated with calcite. Our original microprobe analyses of this specimen had shown that many of the Haversian canal margins are overlain by pure calcite.

It seems likely that published images (Hackett, 1981; Piepenbrink, 1986; Schultz, 1986, p. 89; Garland, 1987; Bell, 1990; Grupe & Dreses-Werringloer, 1992; Jackes, 1992; Grupe *et al.*, 1993) of focal destruction gave an incorrect impression. First, magnification was too low to give a clear picture, and second, images derived only from bone cross-sections most often give a 'cluster of grapes' view. Longitudinal sections may well give a different picture, as suggested by the one longitudinal section published by Bell (1990).

It is quite clear that the foci of destruction are not randomly oriented with regard to bone structure (Jackes, 1990), and we have numerous images showing that they are oriented around the circumferential lamellae in cross-section and generally, though not always, a long axis would be parallel to the long axis of the bone, and hence, of the osteon.

Bacteria cannot be visualized on polished thin sections. We originally examined gold-coated samples from bones and tooth roots which were known, on the basis of thin sections, to have inclusions and to be badly decomposed. While fungal hyphae were observed a number of times (associated with bone vacuities), we were unable to see bacteria, although it became possible—with the Hitachi S-2700 SEM using unpolished, gold-coated bone samples—to identify areas that had been attacked by bacteria (Schultz, 1986 published a similar image, with the destruction attributed to *Streptomyces*).

The very first description of destructive foci seems to have been published by Salomon & Haas (1967), who identified 'granular bodies' in archaeological bone from Israel. They described enigmatic bodies containing bone mineral but differentiated from normal bone because they were not PAS-positive (period acid Schiff stain for glycoproteins). They thus suggested that, in these areas, organic matter was being replaced by mineral. Jackes (1990) sought to elucidate the changes but, apart from proposing that the 'granular bodies' contained bone reprecipitated by bacteria, had barely advanced beyond the knowledge of 1967.

The images produced by the Hitachi S-2700 SEM certainly confirm that the reprecipitated bone surrounding the vacuoles in a destructive focus (that is, the bone of the bright rim) shows a much greater electron density than that of the unaltered bone.

Analyses were undertaken using the Bence-Albee Analysis formula on results from wavelength dispersive analyses (Tracor-Northern Series II X-ray microanalysis system) with an ARL SEMQ microprobe. Many 1 μ point analyses on carbon coated (150 angstrom carbon coating) thin sections of one mid-femoral cortical sample from Arruda (and using one sample of modern femoral cortex from Calcutta as a control) suggested that the bright rim was more than an edge effect.

In Figure 6, the ratio of calcium to phosphorus calculated from totals (i.e. the relative amount of Ca or P per 24 oxygen) forms the y-axis. The Ca + P values plotted on the x-axis approximate the total percent contribution of calcium and phosphorus to the weight of the sample analysed. Examination of the results of the microprobe wavelength dispersive analyses (using the Tracor Northern Series II X-ray

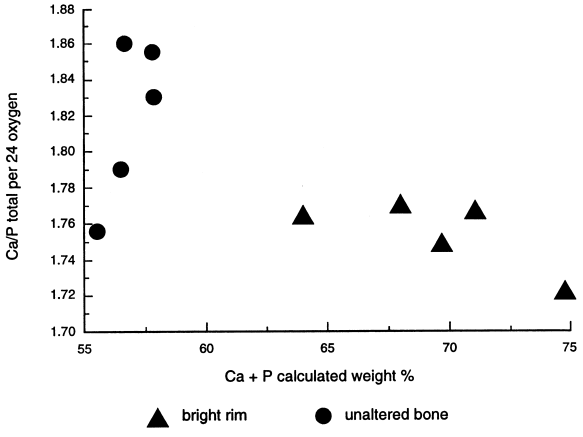

Figure 6. ARL SEMQ microprobe 1 μ point analyses (27.i.92) of Arruda H (femoral sample, core 35), indicating differences in mineral content of bright rim and unaltered bone.

microanalysis system) indicate that there are differences within this one Mesolithic sample of femoral cortex (Arruda H, core 35) between the bright rim and the unaltered bone. The rim has a higher calculated mean weight percent of Ca + P (69.67%), for a higher over-all mineral content than the unaltered bone (56.89%), indicating that the collagen content of the rim is less than that of the unaltered bone.

The assumption of lower collagen content is supported:

1. by reduced birefringence of highly altered areas of bone under polarized light;
2. because Mesolithic bone in a thin section stained with von Kossa's and counterstained with van Geison's indicates a marked difference between rim and non-rim—the deep red of collagen is present only in the areas of non-rim, while the rims show up as bright yellow-white;
3. and because backscattered electron images increase the contrast between the rim and the unaltered bone, confirming the idea of greater mineralization in the rim (Boyce *et al.*, 1990).

Similar analyses to those using the microprobe were done by energy dispersive X-ray analysis (Hitachi S-2700 SEM). The results are equivalent, but not strictly comparable, because different analytical formulae are used by the Link Analyser. The modern control femoral cortex has a mean Ca/P ratio of 1.73 ($n = 5$, S.D. = 0.025) with the output as the normalized percent elemental oxygen. The normalized percent elemental totals for calcium and phosphorus provide a Ca/P ratio which is comparable with that derived from analysis of the same modern femoral thin section using the microprobe (mean = 1.77, $n = 13$, S.D. = 0.027, derived from the calculated totals of calcium and phosphorus per 24 oxygen). Neither result accords exactly with a theoretical Ca/P molar ratio of 1.67, but there is considerable discussion about the way in which actual bone mineral deviates from this (e.g. Misra, 1984, p. 435; Newesley, 1989).

The total mineral content of the modern control sample was analysed on the microprobe and on the SEM. The results were divergent. The microprobe gave a mean calculated weight percentage for calcium of 38.24%, which is exactly as expected (cf. Mazess, 1983, p. 280). The mean for total mineral (Ca + P) of the modern sample was 65.87 (S.D. = 2.08), and this, presumably, includes bone calcium carbonate with the calcium phosphate of mature hydroxyapatite. Given that dry, fat-free, weight-bearing, adult long bone cortex has an ash vs. protein content of 67% and 33%, respectively (Martin and Burr, 1989, p. 81; Mazess, 1983), we assume that the figures derived from the microprobe analysis are reasonable.

However, the SEM results were consistently around 58% for total mineral in the modern control bone (mean = 57.9, S.D. = 0.14, $n = 5$). It is possible that this is calculated from stoichiometry, as it is in such close accord with the theoretical value for hydroxyapatite (which would give a figure of 58.3%; 39.8% Ca, 18.5% P and 1.67 as the mole ratio, derived from the chemical composition of hydroxyapatite with 10 Ca atoms and 6 P atoms). It does not accord with the figures widely quoted in the literature, or our previous analyses, which rely on weight per 24 oxygen (between 65% and 67%). However, a comparable total mineral content (mean = 66.08%, S.D. = 0.36, $n = 5$) can be obtained for the control bone by adjustment of the output method, and this has been used for the following discussion.

While the SEM analyses may introduce difficulties, it is worthwhile to use the SEM rather than the microprobe. The higher image resolution on the SEM gives us confidence that we can differentiate areas of interest. Because we are concerned with relative characteristics within single samples of bone, it is most important that we can differentiate and analyse areas no more than a few microns apart.

From 1985 to 1992, we undertook numerous analyses of Mesolithic bone samples in order to test techniques and methods. These culminated in a series of controlled and consistent SEM linescans in late 1993. Our initial analyses were of single points, and occasionally gave unexplained deviations from expectation. The exact point of analysis is crucial: variations may be introduced by slight misplacements of the point,

if single point analyses are used. While all point analyses were of 1 μ^3, slightly different materials up to 1 μ below the surface may be unintentionally included in an analysis.

Variations may also be a result of electron beam damage to the sample. As the sample charges up, it is no longer possible to see the image clearly (areas of burning can also be identified later as brown points under fluorescing light). When burning is recognized, the results are noted as aberrant, and usually show up in analyses as outliers. Nevertheless, results may be perturbed by sample charging. Backscattered electron imaging at 15 kV reduces charging and beam damage. The Link Analyser Digital Line Scan provides an excellent method of analysing bone chemistry, and allows a control by observation of adjacent points and averaging across points if perturbations are introduced.

The single line scan trajectory illustrated in Figure 7(A) moves across from bright rim, through a small area of relatively unaltered bone, completely surrounded by bacterial decomposition, and back onto a rim, just short of a tunnel. Figure 7(B) shows the grey scale, or the alteration in the electron image, as the scan crosses from the bright rim to the bone and back again.

Data from the linescan illustrated in Figure 7 (Table 4) demonstrate that this particular linescan, which is very clean, so that the 'edge' points can be clearly identified, shows a highly significant difference in mineralization between the rim and the bone ($F = 1.352$ ns, $t = 33.665$, $df = 117$; significant at 0.000).

The bone mineral content of the sample clearly increases across the margin from unaltered bone to rim (shown clearly by the electron image profile in Figure 7(B)). This effect is not random, and it is not a visual edge effect. We have been able to duplicate the profiles in most of similar line scans we have done.

Data from several linescans are illustrated in Figure 8, demonstrating that the mean contribution of Ca + P is higher in the rim than in the unaltered bone (Figure 8(A)), and that there is a higher Ca/P ratio in unaltered bone than in rim (Figure 8(B)), suggesting that the hydroxyapatite is losing calcium relative to phosphorus, perhaps reverting to octocalcium phosphate. Here, we have proof that the rim contains more mineral than the unaltered bone, and that the bright image of the rim actually demonstrates increased density. The reprecipitated bone contains less organic matter than the surrounding unaltered bone. What else it contains is a problem.

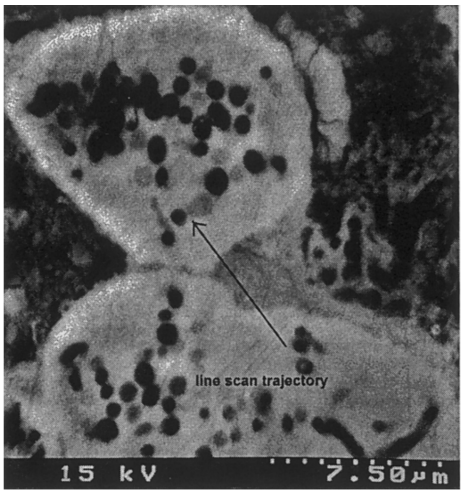

A

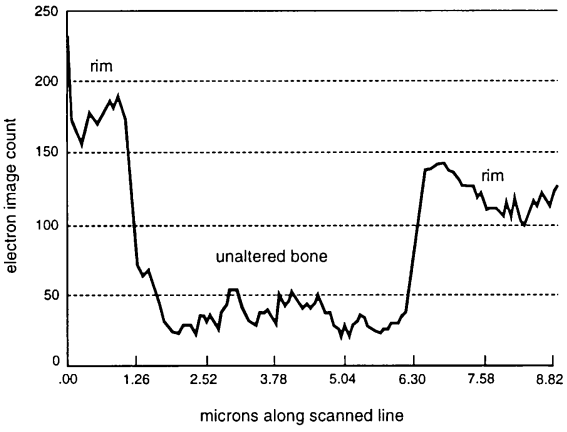

B

Figure 7. Arruda 63 (sample 38), left femoral cortex. (A) Backscattered electron image of polished uncoated thin section showing trajectory of line scan 13 (24.viii.93, Hitachi S-2700 SEM, scale = 7.5 μ). (B) Electron image count of linescan 13: the higher emitted electron intensity count recorded on the *y*-axis of the bright rim areas can be interpreted as indicating greater mineralization.

Table 4. Percent contribution of Ca+P, based on linescan 13 (24.viii.93) for Arruda 63, core 38

Ca+P	Mean	95% limits		S.D.	Minimum	Maximum	*n*
		Lower	Upper				
Rim at start of scan	74.80	74.42	75.18	0.76	73	77	18
Unaltered bone	66.52	66.19	66.85	1.36	64	71	68
Edges	71.06	70.04	72.08	1.22	70	73	8
Rim at end of scan	74.06	73.66	74.46	1.14	72	77	34

One possibility is fluorine. Hassan *et al.* (1977) showed that the fluorine content of fossil bone is increased. Susini *et al.* (1988) suggest that it is bacterially altered bone which increases its fluorine content. Unfortunately, our method of analysis may not show us anything at all. Fluorine may be volatilized into fluorine ions by the heat of the electron beam. The ions are then driven into the sample: 5–7 wt% distributed over quite a large sample is necessary before fluorine content can be determined with precision. The mean calculated weight percent fluorine content of bright rims is slightly higher than that for unaltered bone, according to the microprobe analyses, but this may be an effect of the greater all over mineralization of the rims than the unaltered bone.

SEM point analyses included an analysis of the embedding material (Epoxy) of sample 38, showing that it contained fluorine. A very few other areas in the sample, both rim and unaltered bone, contained small amounts of fluorine; the highest fluorine content, however, was displayed by a cross-sectioned tunnel and an area of convoluted tunnels sectioned longitudinally, suggesting that embedding material was included in the analysis.

A second possibility is strontium. The replacement of calcium by strontium during diagenesis might allow us to do X-ray mapping, indicating the patterning of bone decomposition. In fact, our attempts to demonstrate this have failed: we found virtually no strontium except in exogenous material, where energy dispersive analyses occasionally showed around 700 ppm strontium (0.07 per 24 oxygen).

Our microprobe results suggest that strontium is highest periostially, and in the calcite which fills cracks, Haversian canals and lacunae. While the mean strontium level is higher in altered than unaltered bone, it is likely to be an effect of greater mineralization. The error range is enormous at the levels that we are getting, and for this reason, our microprobe results are inconclusive and we have not been able to achieve analysable results from the SEM. We support the conclusions of Kyle (1986) that strontium distribution parallels silicon and magnesium distribution and is associated with exogenous calcite, not with bone.

We are, then, unable to say anything about the chemical constituents of the rims except that the protein has been selectively removed from the reprecipitated bone, and that the Ca/P ratio is significantly, but slightly, lowered.

It should be made clear that we are unable to analyse the organic fraction of bone using the methods outlined above—the atomic weights are too low. We assume the x-axis in Figure 6 reflects the degree to which the sample is made up of inorganic materials. Thus, we interpret our results to mean that bone with the greatest amount of bright electron image rim will contain the least amount of collagen. The collagen content of our archaeological bone is reduced from 20 or 25% in life (Sandford, 1992; Schoeninger & Moore, 1992) to a mean of 5.4% ($n = 22$). The C/N ratio of collagen in life is about 3, while that from our archaeological bone is higher, showing a relationship between collagen preservation and an increase in the C/N ratio. Carbon is increased relative to nitrogen as collagen is degraded and removed (Child, 1995a, states that C/N does not change until 97% of the collagen has been lost from bone, but our data do not support that).

As previously noted, the density of our archaeological bone is lower than it should be in life (mean = 1.51, $n = 105$, adults cf. 1.8–2 g/cc). In fact, we have a weak association between porosity and density: the more porous the bone in the periosteal third, the lower the density of

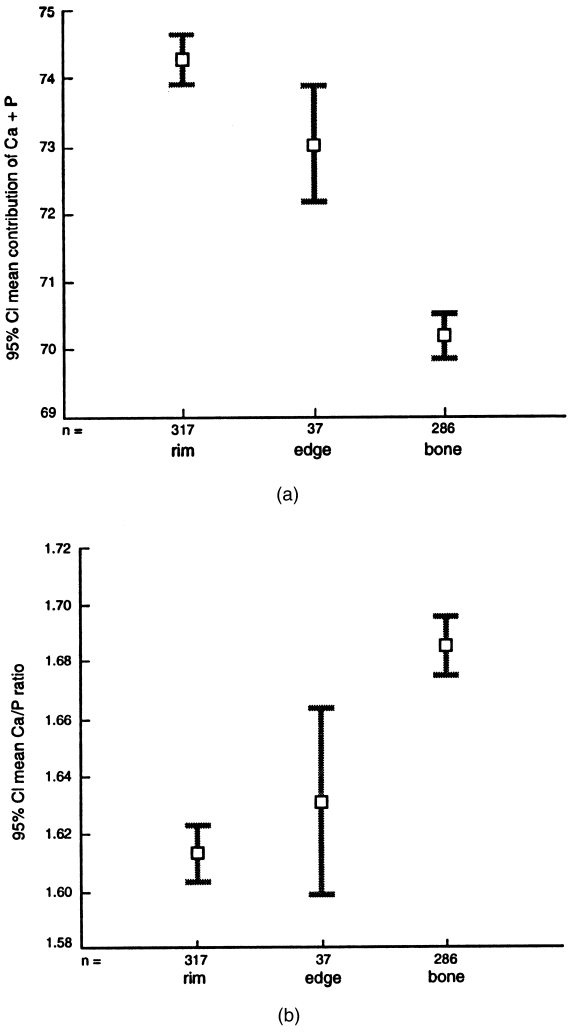

Figure 8. Graphic representation of data from a series of linescans, illustrating the significance of the difference between unaltered bone and bright rim: edge here refers to the margins between the bone and rim, where it is possible that the analysis is sampling both unaltered bone and bright rim. (A) mean and 95% confidence interval of total contribution of calcium and phosphorous; (B) mean and 95% confidence interval of Ca/P ratio.

the specimen. This is the opposite of what happens in living bone (density increases as porosity increases during life) and it suggests that porous bone on the outer surface gains exogenous $CaCO_3$. Bone mineral without collagen should actually have a density of 3 g/cc (Mazess, 1983). The intimate relationship of matrix and periosteum is evident on all our thin sections, so it is clear that bulk samples will include exogenous calcite (efforts to remove exogenous calcite with triammonium citrate resulted in sample destruction).

We used XRD to compare the modern bone sample with two samples of archaeological bone from Moita and Arruda (Figure 9). Our results confirm similar studies (Kyle, 1986; Schoeninger *et al.*, 1989; Sillen, 1989) in showing that the major difference between modern and archaeological bone mineral is the addition of $CaCO_3$ to the latter.

The XRD pattern peaks are more intense and less diffuse in the archaeological samples than in the modern one. The peaks become sharper with increasing crystal size, thus, the broader peaks of modern bone indicate small crystals (Kyle, 1986), while the sharper peaks of the Mesolithic bones indicate larger crystals. Nielsen-Marsh & Hedges (1999) discuss an increase in crystal size (i.e. increased crystallinity) as a consequence of alteration in bioapatite resulting from the removal of collagen (see also Sillen, 1989, p. 215). This is in accord with other research (e.g. Tuross *et al.*, 1989), showing that the hydroxyapatite crystals in fossil bones are altered postmortem into large plate-like crystals 0.25–0.35 μ in length (Susini *et al.*, 1988), which are said to have carbonate inclusions in the lattice.

Hedges & Millard (1995) point out that there is a rather poor understanding of the changes in crystallinity in buried bone (but they do not refer to microbial destruction). Because an increase of carbonates in experimental bone mineral causes apatite crystals to become smaller (LeGeros *et al.*, 1967), it is not at all clear what is happening in Mesolithic bone with regard to carbonates. The bone mineral may be more soluble, the removal of organic matter may make the bone more liable to dissolution (Sillen, 1989). The altered rims are moving towards a calcium salt, which has a lower Ca/P ratio and may be less stable than the unaltered bone. Although there is usually every sign that the rims are very stable, we find that in bone samples which are highly decomposed and with many overlapping destructive foci, some rims are merely narrow remnants (Hackett, 1981 records the removal of redeposited bone mineral).

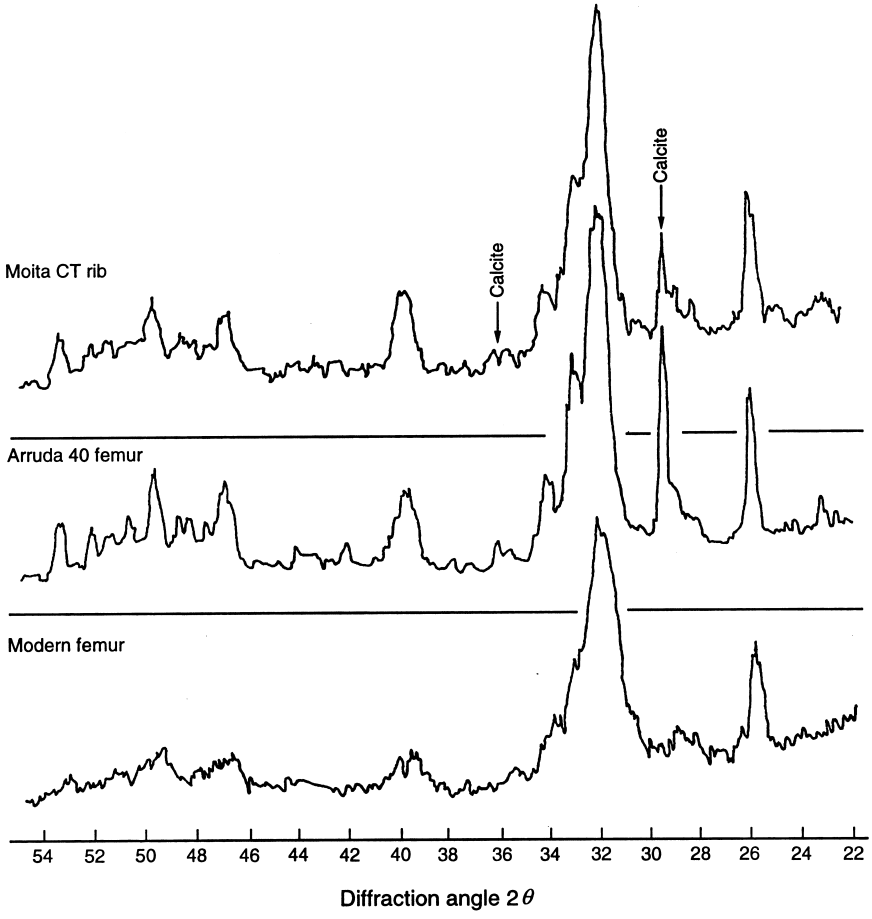

Figure 9. X-ray diffraction patterns of modern control bone and Mesolithic bone samples.

It is unclear whether the rim crystals may actually be small, thus providing a greater surface area liable to dissolution. Our images of unpolished bone at × 8000 to × 20 000 indicate that the large flake-like structures are general in buried bone; however, we have some indications that the rim bone contains smaller crystals (examination at × 8000 of a gold-coated sample).

The basic question is 'what do the bacteria actually do?'. The organic component of bone is stable, except under conditions favourable to microorganisms (Newesley, 1989, p. 244), which indicates that it is microbial action that lowers the collagen content of buried bone. As Child (1995b, p. 168) has said, 'Bone collagen is insoluble . . . and requires special enzymes (collagenases) for its hydrolysis'. Herrmann and Newesley (1982) argued that microbial activity results in acid microenvironments which degrade hydroxyapatite to brushite.

Clostridium histolyticum grows optimally at 37°C and 8.5 pH. Lower temperatures may be tolerated well and higher pH may assist growth at temperatures close to 25°C. A number of enzymes are produced extracellularly, which hydrolize the peptide bonds in a variety of proteins. The various collagenases are the best known—they literally liquify gelatin. These bacteria can live on glycine (which is the important amino acid in collagen) and water alone, in the presence of selenium (zinc and manganese may help). In the presence of calcium, collagenase binds to collagen and reduces it to acid-soluble peptides. The bacterial products are NH_3 (a form of ammonia), acetate (acetic acid),

CO_2 and traces of other acids (formate, lactate, succinate, butyric) (Sneath, 1986; Lebertz & Andreesen, 1988; Minton & Clarke, 1989).

Collagenase will not function at a pH much lower than 6: in fact, it is irreversibly inactivated. So, it is logical that the bacterial acid formation be neutralized by ammonia production. Weak acids such as acetic and butyric cause increased membrane permeability. The diffusion of the acid across the bacterial cell membrane results in acidification of the interior of the cell and the eventual collapse of the membrane pH gradient (i.e. across the membrane between the cell interior and exterior), and even small increases in the acid concentration can result in inhibition of growth. If acidification becomes too great, metabolism ceases and cell viability is lost. We can expect, then, that homeostatic mechanisms should exist to maintain a fairly high pH, but we could also expect that bacterial growth will eventually be such that the whole colony will become too acid—for example, if the colony comes to an obstruction such as the cement line of the osteon (Hackett, 1981 is self-contradictory on this point). Cement lines have a high Ca/P ratio and can be extremely highly mineralized (Ricqlès *et al.*, 1990), but with lower Ca and P content, and a high sulfur content (Martin & Burr, 1989, p. 50). It is reasonable then to view one Haversian system as a fairly closed world for bacteria.

Lowered pH in the reprecipitated bone may be responsible for loss of bright rims in those thin sections which have a great deal of bacterial degradation. Our experiments with decalcification show that even weak solutions of mild acids like formic and acetic cause major destruction of the Mesolithic bone mineral.

We conclude that the Mesolithic bone is partly comprised of bacterially reprecipitated mineral which has had collagen removed. It is possible that the major alteration in the reprecipitated bone mineral is an increased amount of carbonates, leading to greater solubility. Following Herrmann & Newesley (1982), we might suppose that the hydroxyapatite has been converted to octocalcium phosphate which is stable at pH 6–7 rather than the 7–7.5 required for hydroxyapatite. We certainly see no evidence of the brushite identified in several burial conditions.

Figure 10 summarizes our discussions so far. The thin section of Arruda 63 sample 38 was characterized during examination (by transmitted light, fluorescing and polarizing microscopy) as having the 'cloudy, foggy or ashy' overlay that characterized most of our samples, making it impossible to undertake age assessment using osteon counts. Nevertheless, the sample was assessed as being better than most in that it had two midcortical fields which could be examined, so sample 38 was used during the final examination by the Hitachi S-2700 SEM. Figure 10 demonstrates the degree to which bone can be destroyed by bacterial action, with colonies cross and longitudinally sectioned. The colonies abut against one another, and there is even some indication that previous rims may be destroyed (an average rim is 2.5 μ across, based on 12 measurements of clearly present and separate rims, but, in several areas, the rims are 7–9 μ, apparently where two rims are adjacent). Some colonies appear to have no rims at all. The smaller crystals assumed to make up the rims would have a larger ratio of surface area to volume, and would thus be more soluble than unaltered bone. In this image, there remains only one reasonably intact patch of unaltered bone which, at 26×12 μ, is no more than

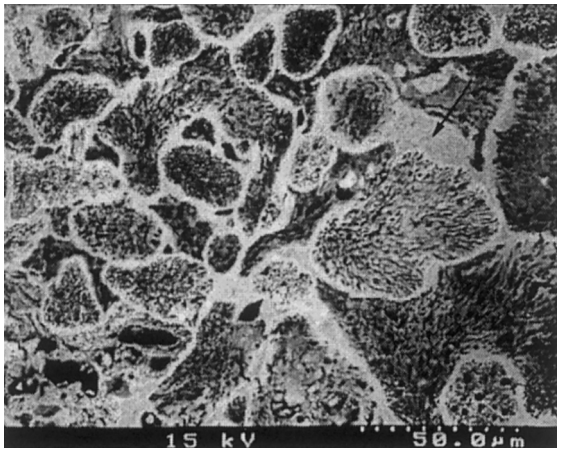

Figure 10. Backscattered electron image illustrating extent of microbial destruction of bone microstructure. The arrow points to the only remaining unaltered bone (Arruda 63, sample 38, left femoral cortex. Hitachi S-2700 SEM, polished uncoated thin section, 24.viii.93, scale = 50 μ).

about 1% of the total area of the image. Nevertheless, some elements of bone microstructure remain: osteonal lacunae can be identified, the largest about 10.5×4 μ.

Figure 10 shows a detail of a thin section which would no doubt be generally characterized as one of 'poor histology' (cf. Hedges *et al.*, 1995, Figure 2). It is unfortunate then, that this thin section is fairly typical of our Mesolithic and Neolithic samples, and it is clear that our understanding of palaeohistology will progress most when we work at the level of a few microns. Hedges *et al.* (1995) characterize the 'foci' as 'nodules', which may or may not become 'holes', but have the same Ca/P ratio as normal bone based on electron microprobe and XRD analyses. We can now understand much more clearly the exact nature of the destructive foci which lead to 'poor histology'.

Experiments on modern bone

The next step in our attempt to understand microbial destruction of bone was the inoculation of the modern bone sample analysed previously with *Clostridium* and other collagenase producing bacteria.

C. histolyticum was not available to us because of the biohazard, so experiments were performed on UV sterilized modern human femoral cortex (details of method available from RS). Four bone slices were checked for anaerobic and aerobic contamination and then placed in a meat broth: three of the bone samples were incubated with bacterial cultures, *C. sporogens*, *C. perfringens* and *C. septicum*. All four cortical samples were stored for seven months before being fixed with formaldehyde.

With *C. perfringens* and *C. septicum*, the bone remained unaltered by the bacteria. With *C. sporogens*, however, the bone surface had dissolved, leaving on the surface sheet-like connective tissue fibres from the meat medium. The bone structure had disappeared into a mass of craters (Figure 11).

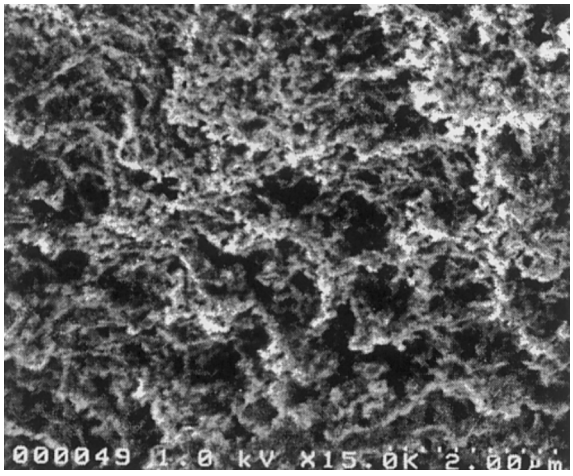

Figure 11. Modern femoral cortical sample incubated for 7 months with *Clostridium sporogens* (Field Emission SEM, Hitachi S-4100, 30.vi.93, image 49 at 1 kV, scale = 2 μ).

We did not succeed in duplicating the effect of the bright rims, honeycomb and streaming tunnelling that we had seen in the polished carbon-coated thin sections of archaeological bone. We, therefore, re-examined the archaeological bone using Field Emission SEM (Hitachi S-4100) which allows the use of unembedded, unpolished, uncoated bone fragments at a very low accelerating voltage (e.g. 1 kV), higher resolution and greater magnification.

The use of thin sections had led to two problems: (1) The 0.25 μ diamond paste used to polish the sections left scratches, which made it difficult to see features in the microprobe; (2) carbon coating (needed for viewing in the microprobe) did not prevent charging of areas being analysed, leading to aberrant results and obscured images. A major difficulty seems to have been the uneven application of carbon coating, a result partly of the use of Portuguese microscope slides, which are smaller than North American ones.

On the other hand, when unpolished bone samples were coated with gold to avoid charging, we were unable to identify even inclusions we knew were there. For example, we knew there was fungal contamination of Furninha bone, because it was visible with transmitted light microscopy, but this was completely obscured by gold coating. We then tried using anti-static spray, but this did not avoid charging. Field Emission SEM (Hitachi S-4100) allowed us to bypass these problems, and gave a

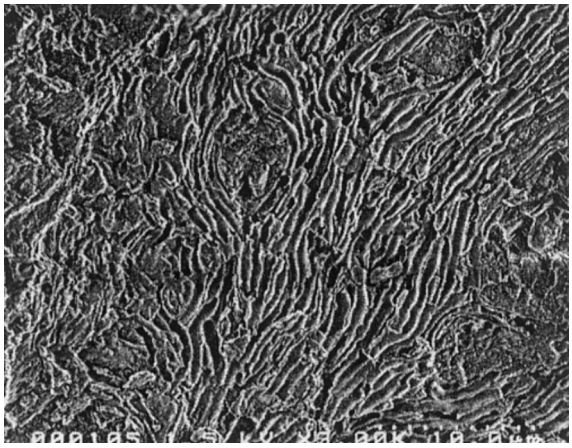

Figure 12. Fragment of a rib from Moita 4. Bacterial tunnelling has been transected lengthways (Field Emission SEM, Hitachi S-4100, 18.viii.93, image 105 at 1.5 kV, scale = 10 μ).

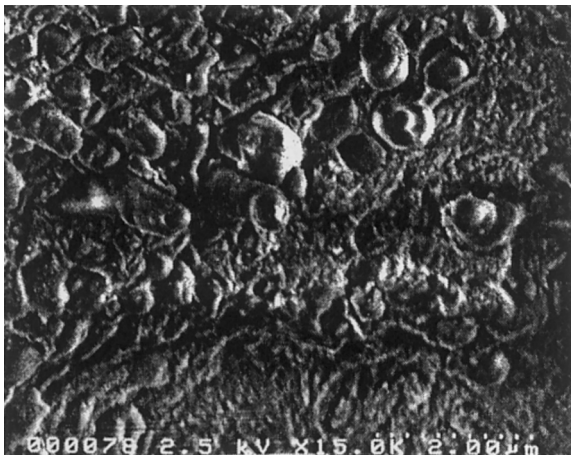

Figure 13. Snapped thin section of left anterior mid femoral cortex (Arruda 35, sample 34), just below the mid shaft. Bacterial tunnels have been broken across showing endocasts emerging from the break at the margin of, but not within, an Haversian canal (Field Emission SEM, Hitachi S-4100, 17.vii.93, image 78 at 2.5 kV, scale = 2 μ).

very clear picture of tunnelling (Figure 12 and Jackes, 2000).

The longer tunnels in Figure 12 are about 10 μ in length, and are streaming around areas untouched by bacteria, the central untouched area on the image being almost 5 μ (500 nm) across. This is at least ten times too small for an Haversian canal. The untouched areas are perhaps an appropriate size for portions of longitudinally sectioned rib lacunae. In the modern control femur we measured six lacunae at $\times 1000$, all of irregular shape, but generally 2–3 μ across. We also measured a longitudinal view of Arruda 9025 (sample 47) using the Hitachi S-4100 at $\times$ 90. These gave us a sample of 24 measurements across lacunae (mean = 2.8 μ) and 27 measurements of lacunae depth (mean = 10.6 μ). The untouched areas are closely set, but, as the minimum distance between lacunae on sample 47 is 8.5 μ, this interpretation is not impossible, though the orientation is not entirely appropriate (canaliculi are smaller—modern control bone, six canaliculi measured, 1 μ across). In the centre right of Figure 12, an endocast about .65 μ is pulling away from a tunnel.

Figure 13 presumably represents endocasts of tunnels, rather than the true form of the bacteria, as the morphology differs from one to another (further end morphologies are shown in Jackes, 2000).

Conclusion

Our research demonstrates that microbial destruction of the structure of archaeological bone can be a serious impediment to analysis of the characteristics of the population represented by those skeletal remains. If osteon counts cannot be used to establish accurate ages of individuals, then the problems of palaeodemographic reconstruction, discussed by Jackes (1992, 2000) and others, become all the more difficult to resolve. But there is certainly scope for other types of studies that allow the use of mid-cortical, rather than periosteal bone, and in which calcite infilling and microbial tunnelling does not prejudice the measurement of porosity. We are continuing further analyses, including work on tetracycline labelling of what appear to be growth arrest lines (Palmer, 1987; Lubell *et al.*, 1994). Questions remain as to the nature of degraded collagen and its bearing on bone chemistry studies (Balzer *et al.*, 1997; Turban-Just, 1997), although our work presents a coherent picture, indicating that the stable isotope data are not being biased by poor results (Lubell *et al.*, 1994). Subsequent work on Portuguese material continues to confirm the picture, indicating that choice of samples and a reasonable sample size are important to obtaining credible results. Our work also

shows that we do not, as yet, have studies at fine enough levels of analysis to make definitive statements about structural and chemical changes resulting from bacterial action upon bone. It is not sufficient to do bulk analyses. Further work aimed at elucidating the details must be done at the micron level.

Acknowledgements

We thank Dr M.M. Ramalho of the Serviços Geológicos de Portugal for permission to study collections in his care, and Dr João Zilhão, Instituto Portugues de Arqueologia, for allowing us to analyse samples from Caldeirão and Feteira. The 1984 series of samples was removed by Dr G. Weih in 1984 at field laboratories set up in Portugal, and processed in Edmonton by E. Palmer (methods described in detail in Palmer, 1987). The 1986 series was removed in Lisbon by José Antonio Severino Rodrigues, who processed the samples for microscopic analysis at the Instituto de Investigação Científica Tropical through the courtesy of the late Dr. Miguel Ramos. Full details of the methods used are available from Jackes. Work on thin sections was done in Edmonton by several technicians in the Department of Geology at the University of Alberta, and especially by Denis Carmel (Oral Biology, University of Alberta), who experimented extensively in attempts to produce readable thin sections. The paper was completed while MJ and DL were Visiting Fellows in the School of Human and Environmental Studies, University of New England, Armidale, NSW. Our thanks to all our colleagues there for their generosity and hospitality and especially to Iain Davidson (Head of School), Mike Roach who prepared the final versions of the figures, and to the staff of the Armidale-Dumaresq Recycling Depot who allowed us to save this paper from the last of a series of misadventures. We acknowledge here the important and original contribution of Esther Palmer, whose death in July 1999 has deprived us of a colleague and friend, unparallelled in her unselfish enthusiasm and dedication. Finally, we are grateful to the Social Sciences and Humanities Research Council of Canada (410-84-0030 and 410-86-2017) and the University of Alberta.

References

Aiello L, Molleson T. 1993. Are microscopic ageing techniques more accurate than macroscopic ageing techniques? *Journal of Archaeological Science* **20**: 689–704.

Balzer A, Gleixner G, Grupe G, Schmidt H-L, Schramm S, Turban-Just S. 1997. In vitro decomposition of bone collagen by soil bacteria: the implications for stable isotope analysis in archaeometry. *Archaeometry* **39**: 415–429.

Baud CA, Lacotte D. 1984. Étude au microscope électronique à transmission de la colonisation bactérienne de l'os mort. *Comptes Rendus Académie des Sciences, Paris* **298**: 507–510.

Bell LS. 1990. Palaeopathology and diagenesis; an SEM evaluation of structural changes using backscattered electron imaging. *Journal of Archaeological Science* **17**: 85–102.

Bergot C, Bocquet J-P. 1976. Étude systématique de l'os spongieux et de l'os cortical du femur et de l'humerus en fonction de l'âge. *Bulletins et Mémoires de la Société d'Anthropologie de Paris (Série XIII)* **3**: 215–242.

Bocquet-Appel J-P, Almeida Tavares de Rocha MA de, Xavier de Morais MH. 1980. Peut-on estimer l'âge au décès à l'aide du remaniement osseux? *Biométrie Humaine* (Paris) **XV**: 51–56.

Boyce TM, Bloebaum RD, Bachus KN, Skedros JG. 1990. Reproducible method for calibrating the backscattered electron signal for quantitative assessment of mineral content in bone. *Scanning Microscopy* **4**: 591–603.

Child AM. 1995a. Microbial taphonomy of archaeological bone. *Studies in Conservation* **40**: 19–30.

Child AM. 1995b. Towards an understanding of the microbial decomposition of archaeological bone in the burial environment. *Journal of Archaeological Science* **22**: 165–174.

Feik SA, Thomas CDL, Clement JG. 1997. Age-related changes in cortical porosity of the midshaft of the human femur. *Journal of Anatomy* **191**: 407–416.

Garland AN. 1987. A histological study of archaeological bone decomposition. In *Death, Decay and Reconstruction*, Boddington A, Garland AN, Janaway RC (eds). Manchester University Press: Manchester; 109–126.

Grupe G. 1995. Preservation of collagen in bone from dry, sandy soil. *Journal of Archaeological Science* **22**: 193–199.

Grupe G, Dreses-Werringloer U. 1992. Decomposition phenomena in thin sections of excavated human remains. In *Histology of Ancient Human Bone: Methods and Diagnosis*, Grupe G, Garland AN (eds). Springer Verlag: Heidelberg; 29–36.

Grupe G, Dreses-Werringloer U, Parsche F. 1993. Initial stages of bone decomposition: causes and consequences. In *Prehistoric Human Bone Archaeology at the Molecular Level*, Lambert JB, Grupe G (eds). Springer Verlag: Heidelberg; 257–274.

Hackett CJ. 1981. Microscopical focal destruction (tunnels) in exhumed human bones. *Medicine Science and the Law* **21**: 243–265.

Hassan AA, Termine JD, Haynes CV. 1977. Mineralogical studies on bone apatite and their implications for radiocarbon dating. *Radiocarbon* **19**: 364–374.

Hedges REM, Millard AR. 1995. Bones and groundwater: towards the modelling of diagenetic processes. *Journal of Archaeological Science* **22**: 155–164.

Hedges REM, Millard AR, Pike AWG. 1995. Measurements and relationships of diagenetic alteration of bone from three archaeological sites. *Journal of Archaeological Science* **22**: 201–209.

Herrmann B, Newesley H. 1982. Dekompositionsvorgänge des Knochens unter langer Liegezeit. 1. Die mineralische phase. *Anthropologische Anzeiger* **40**: 19–31.

Jackes M. 1990. Diagenetic change in prehistoric Portuguese human bone (4000 to 8000 BP). Symposium on Bone Chemistry, Canadian Association for Physical Anthropology, 18th Annual Meeting.

Jackes M. 1992. Paleodemography: problems and techniques. In *Skeletal Biology of Past Peoples: Research Methods*, Saunders SR, Katzenberg MA (eds). Wiley-Liss: New York; 189–224.

Jackes M. 2000. Building the bases for paleodemographic analysis: adult age and sex determination. In *Biological Anthropology of the Human Skeleton*, Katzenberg MA, Saunders SR (eds). Wiley-Liss: New York; 407–456.

Jackes M, Barker T, Wayman M. 1992. Bacterial effects on human bone from archaeological sites. Canadian Association for Physical Anthropology, 20th Annual Meeting.

Jackes M, Lubell D. 1992. The Early Neolithic human remains from Gruta do Caldeirão. In *Gruta do Caldeirão—O Neolítico Antigo*. Trabalhos de Arqueologia, 6, Zilhão J (ed.). Instituto Português do Património Arquitectónico e Arqueológico: Lisboa; 259–295.

Jackes M, Lubell D. 1999. Human biological variability in the Portuguese Mesolithic. *Arqueologia (Porto)* **24**: 25–42.

Jackes M, Lubell D, Meiklejohn C. 1997. Healthy but mortal: human biology and the first farmers of Western Europe. *Antiquity* **71**(273): 639–658 (original text plus supplementary material available at http://intarch.ac.uk/antiquity).

Kyle JH. 1986. Effect of post-burial contamination on the concentrations of major and minor elements in human bones and teeth—the implications for paleodietary research. *Journal of Archaeological Science* **13**: 403–416.

Lazenby R. 1986. Porosity-geometry interaction in the conservation of bone strength. *Journal of Biomechanics* **19**: 257–258.

Lebertz H, Andreesen JR. 1988. Glycine fermentation by *Clostridium histolyticum*. *Archives of Microbiology* **150**: 11–14.

LeGeros RZ, Trautz OR, LeGeros JP, Klein E, Shirra WP. 1967. Apatite crystallites: effects of carbonate on morphology. *Science* **155**: 1409–1411.

Lubell D, Jackes M, Schwarcz H, Knyf M, Meiklejohn C. 1994. The Mesolithic-Neolithic transition in Portugal: isotopic and dental evidence of diet. *Journal of Archaeological Science* **21**: 201–216.

Martin RB, Burr DB. 1989. *Structure, Function, and Adaptation of Compact Bone*. Raven Press: New York.

Mazess RB. 1983. Non-invasive bone measurements. In *Skeletal Research: An Experimental Approach*, vol. 2, Kunin AS, Simmons DJ (eds). Academic Press: New York; 277–343.

Minton NP, Clarke DJ. 1989. *Clostridia*. Plenum: New York.

Misra DN. 1984. Surface chemistry of bone and tooth mineral. In *Methods of Calcified Tissure Preparation*, Dickson GR (ed.). Elsevier: Amsterdam; 435–464.

Newesley H. 1989. Fossil bone apatite. *Applied Geochemistry* **4**: 233–245.

Nicholson RA. 1998. Bone degradation in a compost heap. *Journal of Archaeological Science* **25**: 393–403.

Nielsen-Marsh CM, Hedges RM. 1999. Bone porosity and the use of mercury intrusion porosimetry in bone diagenesis studies. *Archaeometry* **41**: 165–174.

Palmer E. 1987. Micromorphology of prehistoric bone from the Mesolithic site of Moita do Sebastião, Portugal. Unpublished MA thesis, Department of Anthropology, University of Alberta.

Pate FD. 1998. Bone collagen preservation at the Roonka Flat Aboriginal burial ground: a natural laboratory. *Journal of Field Archaeology* **25**: 203–217.

Pfeiffer S. 1998. Variability in osteon size in recent human populations. *American Journal of Physical Anthropology* **106**: 219–227.

Pfeiffer S, Lazenby R, Chiang J. 1995. Cortical remodeling data are affected by sampling location. *American Journal of Physical Anthropology* **96**: 89–92.

Piepenbrink H. 1986. Two examples of biogenous dead bone decomposition and their consequences for taphonomic interpretation. *Journal of Archaeological Science* **13**: 417–430.

Ricqlès A de, Meunier FJ, Castanet J, Francillon-Viellot H. 1990. Comparative microstructure of bone. In *Bone*, Hall BK (ed.). Telford Press: Caldwell, NJ; 1–78.

Salomon CD, Haas N. 1967. Histological and histochemical observation on undecalcified sections of ancient bones from excavations in Israel. *Israel Journal of Medical Science* **3**: 747–754.

Sandford MK. 1992. A reconsideration of trace element analysis in prehistoric bone. In *Skeletal Biology of Past Peoples: Research Methods*, Saunders SR, Katzenberg MA (eds). Wiley-Liss: New York; 79–103.

Schoeninger MJ, Moore KM, Murray ML, Kingston JD. 1989. Detection of bone preservation in archaeological and fossil samples. *Applied Geochemistry* **4**: 281–292.

Schoeninger MJ, Moore K. 1992. Bone stable isotope studies in archaeology. *Journal of World Prehistory* **6**: 247–296.

Schultz M. 1986. Die mikroskopische untersuchung prähistorischer skeletfunde: anwendung und aussagemöglichkeiten der differentialdiagnostischen untersuchung in der paläpathologie. Archäologie und Museum: Tagungsberichte zum Paläopathologischen Symposium in Liestal (Baselland) 21.-23.Juni 1984, Band 1. Heft 006, Berichte aus der Arbeit des Amtes für Museen und Archäologie des Kantons Baselland.

Scion Image. 1998. Release Beta 3b. Frederick, Maryland: Scion Corporation. http://www.scioncorp.com, 23 July 1998.

Serviços Geológicos de Portugal. 1969. *Carta Geológica do Quaternário de Portugal na escala de 1/1 000 000* with *Notícia Explicativa* by G. Zbyszewski (1971). Direcção-Geral de Minas e Serviços Geológicos: Lisboa.

Sillen A. 1989. Diagnosis of the inorganic phase of cortical bone. In *The Chemistry of Prehistoric Human Bone*, Price TD (ed.). Cambridge University Press: Cambridge; 211–229.

Sneath PHA (ed.). 1986. *Bergey's Manual of Systematic Bacteriology*, vol. 2. Williams and Wilkins: Baltimore.

Strauss LG, Altuna J, Carvalho E, Jackes M, Kunst M. 1988. New excavations in Casa da Moura (Serra d'el Rei, Peniche) and at the Abrigos de Bocas (Rio Maior), Portugal. *Arqueologia* **18**: 65–95.

Susini A, Baud CA, Lacotte D. 1988. Bone apatite crystals alterations in Neolithic skeletons and their relations to burial practices and soil weathering. *Rivista di Antropologia (supplemento)* **LXVI**: 35–38.

Turban-Just S. 1997. Zum biogenen Abbau menschlicher Knochenkollagene. *Anthropologische Anzeiger* **55**: 131–141.

Tuross N, Behrensmeyer AK, Eanes ED. 1989. Strontium increases and crystallinity changes in taphonomic and archaeological bone. *Journal of Archaeological Science* **16**: 661–672.

Uytterschaut HT. 1985. Determination of skeletal age by histological methods. *Zeitschrift fur Morphologie und Anthropologie* **75**: 331–340.

Uytterschaut HT. 1992. Human bone remodeling and aging. In *Histology of Ancient Human Bone: Methods and Diagnosis*, Grupe G, Garland AN (eds). Springer Verlag: Heidelberg; 95–109.

Yoshino M, Kimijima T, Miyasaka S, Sato H, Seta S. 1991. Microscopical study on estimation of time since death in skeletal remains. *Forensic Science International* **49**: 143–158.

Zilhão J. 1984. *A Gruta da Feteira (Lourinhã): Escavação de salvamento de uma necrópole neolítica*. Trabalhos de Arqueologia 1. Instituto Português do Património Cultural: Lisboa.

Zilhão J. 1992. *Gruta do Caldeirão. O Neolítico Antigo*, Trabalhos de Arqueologia 6. Instituto Português do Património Arquitectónico e Arqueológico: Lisboa.

